Original Research Article

Friction and Wear Behaviour of Plasma Sprayed Fly Ash Added Red Mud Coatings

Abstract: The present investigation aims at evaluating the effect of fly ash addition on sliding wear behaviour of pure red mud. Plasma sprayed coatings composed of red mud and varying percentage of fly ash were considered for the wear behavior study. Plasma spraying technique was used with varying levels of ~~energy for the purpose of spraying. The different levels of operating power maintained were~~power, namely 6, 9, 12 and 15 kW. Investigations of the coatings focused on ~~the basis of some~~ tribological properties like sliding wear behaviour, wear morphology, wear mechanism and frictional force. Experimental investigations also included the effect of varying percentage of fly ash on dry sliding wear behaviour of pure red mud. Fly ash with 10, 20 and 50 % by weight was mixed with red mud and sliding wear test performed using pin on disc wear test machine. The wear test was performed for sliding distance up to 942 m with track diameter of 100 mm and at sliding speed of 100 rpm (0.523 m/s); applying normal load of 10 N for a maximum duration of 30 minutes. The ~~plots pertaining to the~~ variation of wear rate and frictional force with that of sliding distance and time ~~has been~~is presented. Significant wear resistance ~~being~~ was visible with the addition of fly ash due to increase in bond strength and dense film at the interface. Wear rate decreases with operating power up to 12 kW; thereafter declines ~~initiating~~ due to other dominating factors~~parameters~~.

Key words: Red mud; Fly ash; Plasma Coating; Sliding wear; Wear morphology; Frictional force; wear mechanism.

1. INTRODUCTION:

Coating technologies have already gained a promising momentum for the creation of emerging materials in the last few decades. Coatings with ~~some~~ advanced wear properties ~~put a signature of~~ claim~~ing~~ frequent~~for the better~~ use in tribological applications. Plasma spray is one of the most widely used techniques involved in surface modification by ~~augmentation~~ improvement of wear resistance, which may affirm the great versatility and its application to a wide spectrum of materials. The coatings with considerable amount of hardness can protect

against variety of wear mediums including abrasive, adhesive and corrosive. Basically, wear resistantive coatings are fabricated by consideringfrom some common conventional materials like nickel, iron, cobalt and molybdenum based alloys [1-2]. Extensive investigations pertaining toof the erosion wear behavior of plasma sprayed ceramic coatings by using Taguchi Technique being was reported by some experimenters [3]. The tribological properties of traditional manganese phosphate coatings and hBN composite coatings composed of nano hexagonal boron nitride (hBN) in layered manganese phosphate crystals on AISI 1040 steel were being divulgedstudied in some literatures [4].

In retrospection, literatures madeStudies are also available regarding the wear behaviour of WC with 12% Co coatings produced by Air Plasma Spraying method at different standoff distances [5]. Examinations on the basis of the wear behaviour of Mo and Mo+NiCrBSi thermally sprayed coatings being were performed for the application as next generation ring face coatings [6]. Almost all plasma sprayed ceramic coatings portrayed featured favorable tribological performance in linear contact at high temperatures: high anti-wear resistance and easy to be lubricated owing to the oil storage of pores in coatings [7-9]. But needful to say, plasma sprayed ceramic coatings exhibit some failure mechanisms during sliding such as plastic deformation, brittle fracture and polishing effects [10], which in turn demands a few additives, which could reduce the friction and wear of plasma sprayed ceramic coatings [11].

Several factors may influence the tribological behaviour of a coated surface, suchramified as: the geometry of the contact, including macro geometry and topography of the surfaces; the material characteristics; basic mechanical properties as well the microstructure and finally the operating parameters controlling the coating deposition [12].

Red mud as an industrial waste material is considered to be the material of choice for coating applications. It is behooved to mention here that, red mud in present decade should be considered as an alternative wealth for replacing some conventional expensive coating materials. Utilization of red mud and its implications made is available in literature [13] in great details. Few results on the basis of wear behavior of red mud were being reported by some researchers. In addition to the above, morphology and solid particle erosion wear behaviour of red mud and fly ash composite were being availablestudied in literature [14]. Characteristics of plasma sprayed pure red mud coatings were being reported in [15]. Red mud as filling material is also found to be the wear enhancing agent for metals [16]. Tribological aAspects of tThermally sSprayed rRed mMud-fFly aAsh and rRed mMud-Al cCoatings on mMild sSteel was reported [17]. Data pertaining to the sliding wear behavior of fly ash based red mud composite coatings are not abundant and need to be addressed. The

present investigation ~~is an attempt in a direction~~aims to evaluate the wear behavior of varying percentage of fly ash with pure red mud coating at different operating power subjected to normal laboratory conditions. This paper may pave the path for ~~furthering~~ extending the study to throw ~~some further~~more light on fly ash based red mud coatings.

2. MATERIALS AND METHODS OF EXPERIMENTATION

2.1 Preparation of coating powder

The present experimental work included the preparation of coating powder ~~considering~~ from the raw materials as red mud and fly ash powders. The powder mixture ~~concomitants~~ of red mud and different percentage of fly ash was ~~being~~ prepared ~~and mixed~~ using V-shaped drum mixer. In addition, pure red mud powder was also ~~considered~~ used as coating material for the ~~sake of~~ comparison on the basis of percentage of fly ash addition. Coating of the various combinations of mixed powders was conducted on one side cross section of the mild steel substrate. Data ~~pertaining to~~in Table 1 ~~contains~~shows~~~~ the different ~~combinations of the~~ mixtures chosen for plasma spraying.

Table. 1 Powders used for coating deposition.

Sl.No.	Coating m~~M~~aterial	Mixture c~~C~~omposition (b~~B~~y weight %)
1	Red m~~M~~ud (RM)	100
2	Red m~~M~~ud + f~~F~~ly a~~A~~sh (FA)	90 + 10
3	Red m~~M~~ud + f~~F~~ly a~~A~~sh	80 + 20
4	Red m~~M~~ud + f~~F~~ly a~~A~~sh	50 + 50

Red mud, as the primary raw material was collected in powder form from National Aluminium Company (NALCO) located at Damonjodi in the state of O~~o~~disha, India. The as-received powder was sieved to obtain particles in the required size range of 80-100 µm. Raw fly ash was collected from the captive power plant of Rourkela steel plant, India and ~~allowed for sieving~~sieved to ~~maintain~~ the same size range as that of fly ash powder. Powders having three different weight ratios of red mud and fly ash (Table 1) were ~~extensively~~ prepared by mixing thoroughly.

2.2 Preparation of substrates

Commercially available mild steel rod was ~~mooted~~ used as source for substrate preparation. The rod was cut to ~~some number of~~ pieces having one particular dimension (l = 40 mm and Ø= 12 mm) each. The specimens were grit blasted from one side cross section (initial roughness 0.03 mm) at a pressure of 3 kg/cm^2 using alumina grits of grit size 60. The

stand-off distance in the shot blasting was kept between 120-150 mm. Then the average roughness of the substrate was ~~reported to be~~ 6.8 µm. The grit blasted specimens were ~~allowed~~ used for plasma spraying after cleaning in an ultrasonic cleaning unit.

2.3 Plasma spraying

The spraying process was performed at the Laser and Plasma technology division of Bhabha Atomic Research Centre, Mumbai, India by adopting conventional atmospheric plasma spraying (APS) set up. The plasma input power was varied from 6 to 15 kW by controlling the gas flow rate, voltage and arc current. The powder feed rate was maintained ~~to be~~ constant at 10 g~~m~~/min by using a turntable type volumetric powder feeder. Plasma generation ~~demanded the suitability by purging~~used ~~Argon~~ argon as primary and ~~Nitrogen~~ nitrogen as secondary gas agent. The mixture of powders were deposited at spraying angle of 90° by maintaining the powder feeding ~~as~~ external to the gun. ~~The properties of the coating are merely depends upon the parameters of spraying process.~~ The operating parameters ~~maintained during~~of the coating deposition process are ~~being tabulated~~shown in Table~~.~~ 2.

Table 2. Operating parameters during coating deposition

Operating p~~P~~arameters	**Values**
Plasma ~~Arc~~ arc ~~Current~~ current (Ampere)	200,225,250,300
Arc ~~Voltage~~ voltage (Volt)	30,40,48,50
Torch ~~Input~~ input ~~Power~~ power (kW)	6,9,12,15
Plasma ~~Gas~~gas (a~~A~~rgon), (litre/min)	20
Secondary ~~Gas~~gas (~~Nitrogen~~nitrogen),(litre/min)	2
Carrie~~e~~r ~~Gas~~gas (a~~A~~rgon) f~~F~~low rate (litre/min)	7
Powder f~~F~~eed r~~R~~ate (gm/min)	10
Torch to base distance (mm)	110
Arc l~~L~~ength r~~R~~ange (mm)	2,3,6,8,11

2.4 Pin on disc w~~W~~ear t~~T~~esting

The above experiment was being conducted in the pin on disc type friction and wear monitor (DUCOM; TR-20-M100) with data acquisition system. The ~~concerned~~ machine was used to evaluate the wear behavior of the coatings against hardened ground steel disc (En-32) having hardness of 65 HRC and surface roughness (Ra) 0.5 µm. The ~~versatility of the~~ equipment ~~lies behind~~is ~~the~~ design~~ed~~ to study the wear behaviour under un-lubricated sliding condition, which occurs between a stationary pin and a rotating disc.

The disc of the machine rotates with the help of a D.C. motor having speed range of 0-200 rpm with wear track diameter 0-160 mm; this~~which~~ can yield sliding speed of 0-10 m/s. Load

is ~~to be~~ applied on the pin (specimen) by dead weight through pulley string arrangement. The system has a maximum loading capacity of 500 N. For the present experimentation, pin specimen was kept stationary perpendicular to the disc, while the circular disc was rotated as shown in Figure 1.

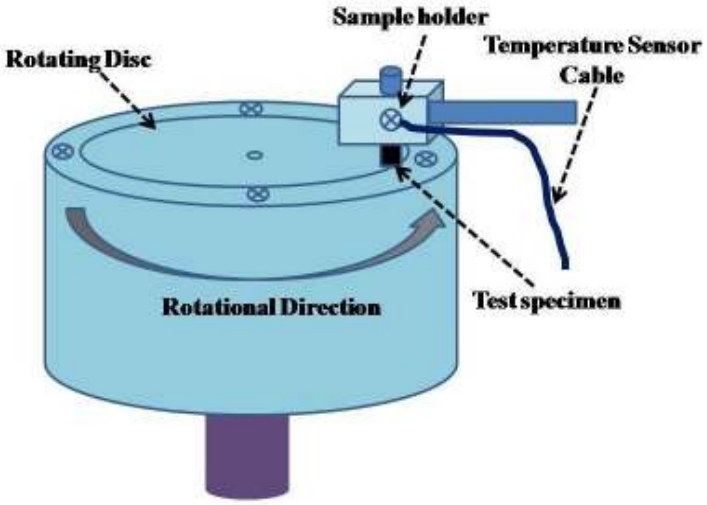

Figure 1. Schematic Representation of Pin on Disc Apparatus

3. RESULTS AND DISCUSSION

3.1 Scanning electron microscopy and c~~C~~ompositional analysis

The characterization of red mud powder involved taking microstructures by the help of s~~S~~canning electron microscope (JEOL; JSM-6480 LV). The micro-structural images captured by SEM (s~~S~~canning electron microscope) and EDS (energy dispersive spectroscopy) analysis of pure red mud powder ~~were being~~are illustrated in Figure 2. EDS experiment was performed by the above SEM with the required attached module. Data presented in Table 3 indicate~~s~~ the weight as well the atomic percentage of elements comprising pure red mud powder. The EDS analysis of red mud revealed the signature of ~~some~~ elements like Fe, Al, Si, O and some other minor constituents. The prominent constituent of red mud was found to be iron with its oxides. The EDS analysis of red mud with 20 % fly ash coatings prepared at 9 kW of operating power is shown in Figure~~.~~ 3. In addition, the analogous elemental analysis relating to Figure ~~-~~3 is reported in Table~~.~~ 4, indicating the increase in silica and iron constituents in the composite coating.

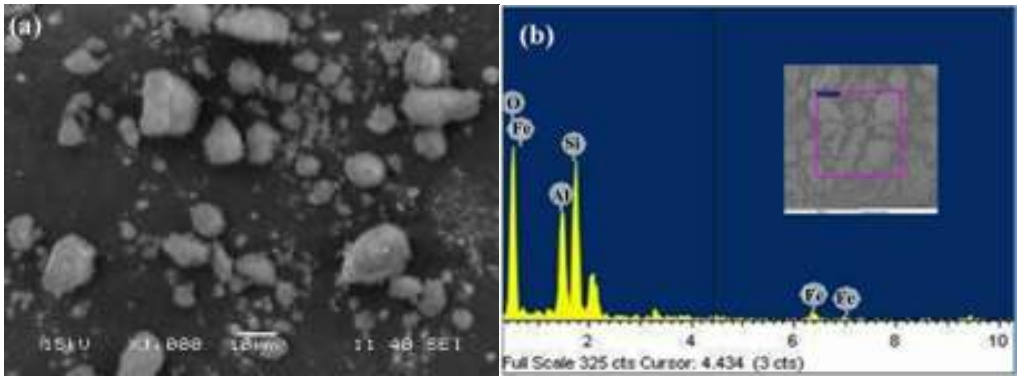

Figure 2. (a) SEM and (b) EDS analysis of red mud

Table 3. Elemental analysis of red mud

Element	Weight%	Atomic%
C K	24.59	33.29
O K	23.65	24.54
Al K	7.41	4.47
Si K	12.21	7.07
Fe K	32.14	30.62
Totals	100.00	

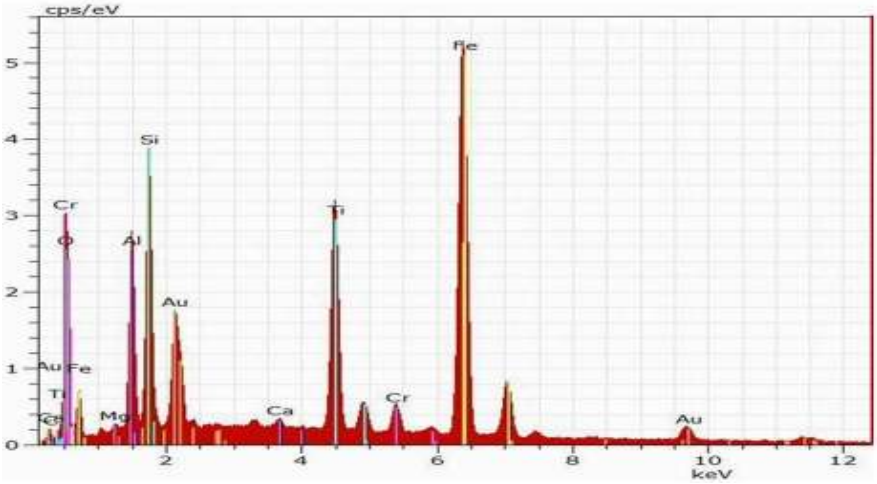

Figure 3. EDS analysis of RM+20 % FA cComposite coating at 9 kW

Table 4.Elemental analysis of RM+20 % FA cComposite coated at 9 kW

Element	Weight %	Atomic %
Fe K	36.13	25.90
O K	21.74	42.61
Ti K	14.02	9.18

Si K	17.10	7.93
Al K	6.59	7.66
Cr K	2.14	1.29
C K	1.99	5.20
Ca K	0.29	0.22
Au K	0.00	0.00
Mg K	0.00	0.00
Totals	100 %	100

3.2 Coating porosity

Image analysis technique was adopted for the measurement of porosity of coating materials. The polished surfaces of various coatings were kept under a microscope (Neomate) equipped with a charge coupled-device (CCD) camera (JVC, TK 870E). Volume of interest (VOIS) image analysis software paid an important role for the determination of porosity. The software can measure accurately the total area captured by the objective of the microscope. Hence the total area and the area covered by the pores are separately measured to report porosity. The "VOIS image analysis software" used in this analysis is being licensed by the authors. The porosity data of three different coatings ~~powders~~ are ~~being tabulated~~shown in Table ~~.~~5. A cross sectional view of red mud coating prepared at 9 kW of operating power was captured by the help of field emission scanning electron microscope (FESEM; Nova Nano SEM-450), as shown in Figure 4.

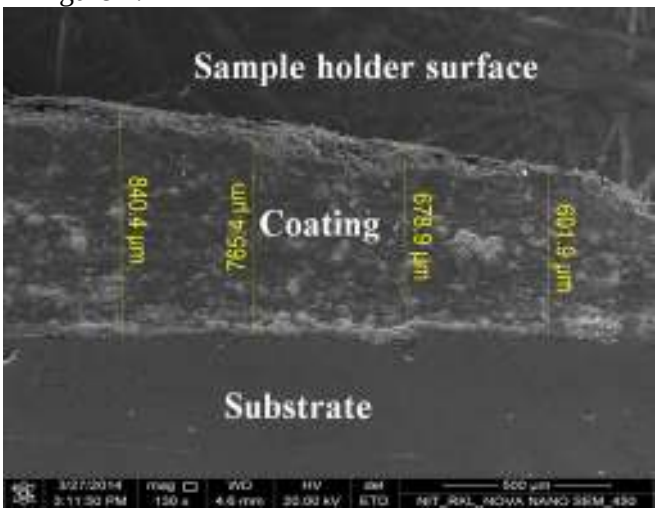

Figure 4. FESEM image of coating c~~C~~ross section of pure red mud at 9 kW

Table 5. Coating p~~P~~orosity for different coating type~~s~~.

Coating m~~M~~aterial	**Plasma t~~T~~orch i~~I~~nput p~~P~~ower (kW)**	**Porosity (%)**

Red mMud	6	12.89
	9	12.02
	12	11.87
	15	13.02
90 % rRed mMud + 10 % fFly aAsh	6	11.52
	9	11.12
	12	10.90
	15	12.98
80 % rRed mMud + 20 % fFly aAsh	6	10.89
	9	10.54
	12	10.17
	15	11.78

Approximately 8-13% porosity range was observed (Table-3) for all three coating materials. Porosity amount was found to be ameliorated in case of all coating compositions prepared at lower (6 kW) and at higher (15 kW) power levels. At 6 kW operating power level, there is poor melting of particles subjected to relatively low plasma gas temperature exhibiting non-uniform mixing of molten particles; which in turn causes reasonably porous coating layer. On the other hand, at highest operating power level (15 kW) the high plasma gas temperature caused faster deposition of molten particles by creating thickened coating layer with less hardness and high porosity.

Porosity level was found to be higher in case of pure red mud compared to the composite coatings ~~pertaining to~~made of the mixture of fly ash and red mud. About 3-10% porosity level was reported for the coatings prepared by conventional plasma spraying [18], which supports the porosity results ~~as~~ obtained in the present investigation.

3.3 Coating hHardness

The polished section of the coatings was put under optical microscope for the microscopic observations, which revealed the presence of three distinguishable different phases, namely dull, white and spotted. The three different distinct phases ~~are allowed for~~were subject to micro indenting to record micro-hardness data with the help of Leitz micro-hardness tTester using 50 Pa (0.493 N) on all samples. The results are summarized in Table ~~.~~6. The three structurally different phases of red mud coatings bear three different ranges of hardness values varying from 488 to 588 HV. Hardness values were found to be enhanced for the ~~composite coatings belonging mixture of~~ red mud and fly ash composite coatings. This result is attributed ~~due~~ to the increased content of alumina and silica in the composition of feed material forming alumino-silicate (mullite phase) during spray deposition [19].

Table 6. Coating ~~Hardness~~ hrdness for different operating power level

Coating ~~Material~~material	Plasma tTorch iInput pPower (kW)	Micro-Hhardness (HV)		
		Dull	White	Spotted
100% ~~Red Mud~~red	6	540	488	496
	9	532	498	511

mud	12	586	513	508
	15	555	502	510
90% Red Mudred mud + 10 % Fly Ashfly ash	6	638	632	628
	9	648	642	636
	12	660	638	628
	15	651	640	632
80 % Red Mudred mud + 20 % Fly Ashfly ash	6	658	649	642
	9	669	658	649
	12	699	689	652
	15	681	681	650
50 % Red Mudred mud + 50 % Fly Ashfly ash	6	696	679	658
	9	682	633	672
	12	726	712	660
	15	719	679	668

3.4 Wear test study

Prior to the starting of the wear testing experiment, the pin and the disc surface of the concerned equipment were polished perfectly with emery papers for better ensuring of smooth contact with the coating samples. Hereafter the surface roughness lessens by a magnitude ofwas reduced to 0.1 µm. The wear tests were carried out as per ASTM G- 99 standard for maximum time period of 30 minutes under un-lubricated condition in a normal laboratory ambience having relative humidity of 40-55% and the temperature range of 20-25°C. The weight of the specimens before and after the wear experiment were being recorded by using electronic weighing machine having accuracy up to second decimal limitof (0.01 mg) for monitoring the mass loss occurrence in the coating samples. Specimens were taken care of in particular forperiodically cleaneding with woolen cloth to avoid entrapment of wear debris and to maintain uniformity in each set of experiments. The test pieces weare cleaned with tetrachloroethylene solution before and after each test. Wear rate was estimated by measuring the mass loss (Δm) ofin the specimen after each test. Wear rate relating to mass loss and the sliding distance (L) was formulated below in equation (1).

$$W_r = \frac{\Delta m}{L} \tag{1}$$

where W_r = wear rate in N/m;

Δm = mass loss in Newton (N);

L = sliding distance in meter (m).

The frictional force (F) was measured directly from the apparatus in ‘kg’ at each time interval.

The wear experiment was carried out at normal atmospheric temperature under a constant normal force of 10 N and a fixed speed of 100 rpm. The track diameter of the equipment was kept at 100 mm. The maximum duration of sliding was 30 minutes, comprising of 10 intervals with each havingof 3 minutes eachof time gap. Each sample specimen was allowed for sliding for distinct time interval.

Initially, the experiment was performed with red mud coated samples and then continued for fly ash based red mud coating composites. Figure 5 illustrates the variation of wear rates with sliding distance for different operating power levels.

The wear results for pure red mud coating operated at 6 kW of operating power being visible in Figure 5 (a) discloseing the variation of wear rate with minimum value of 0.11 N/m to maximum value of 0.45 N/m. The wear rate value was found to be increased from 0.11 to 0.13 N/m for the first 6 minutes of sliding. After a drastic increase from 6 to 12 minutes of duration, tThe wear rate plot assuffirmed a plateau just after a drastic increasing trend from 6 to 12 minutes of duration. The evolution ofplateau in wear rate value may be attributed due to the variation of coating layer property. This is one fact may indicateing the more higher hardness of denser surface of top layer than that of bulk layer. The change of coating property just after 6 minutes of sliding may be due to the coating property variations bearing less hardness of bulk layer.

The wear rate was reduced for fly ash based (10%, 20% and 50%) composite coatings, as being illustrated in Figure 5. Theis wear rate indicative trends of wear rate for fly ash composite coatings are quite similar to thoseat of pure red mud coating. InitSubstantial slow increase in wear rate for the composite coatings was being visible, followed by a drastic increasegain. Henceforth, the wear rate was roughly constant for all composite coating types. The plots pertaining toin Figure 6 represent the variation of wear rates of each coating type with that of sliding distance for different operating power levels.

The effect of operating power level on wear rate is quite interesting. The wear rate is resulted attributing toaffected by the porosity and hardness. The wear rate was found to be enhanceddecrease up to 12 kW and departing resultincrease again slightly for 15 kW. The wear rate for 15 kW was found to be lied between 9 and 12 kW. This might be due to the improper particle to particle bonding and poor stacking to the substrate, which in turn lowered the hardness as well as density due to poor interfacial bond strength. Figure 7 shows the trends of wear rate for all coating materials against operating power level for a particular sliding time (15 minutes).

An experimental study on coating thickness for fly ash and red mud composite with operating power is reported in [19]. An increase in coating thickness with increase in input power to the plasma torch,; up to about 12 kW, is observed and then with further higher input power, no improvement in coating thickness is recorded.

The frictional force (F) in kg was measured directly from the wear apparatus deputed for the present investigation. The graphical representation concerning the variation of frictional forces with that of sliding time is focused onshown in Figure 8, which includes the picture for all coating materials and also for operating power levels considered. As per the observations, maximum frictional force is evidenced for pure red mud coating and being decreasesd with the addition of fly ash, akin to the results as being occurredobserved for the wear rate. An increase in frictional force up to a maximum value of 0.63 kg for pure red mud coating at 12 minute sliding time is observed, followed by a fluctuating wavy response up to 21 minutes, then a constant magnitude up to 30 minutes of sliding.

Figure 9 ~~shows the~~ comparesative ~~study relating~~ frictional forces for the coating composites with 10% fly ash. The frictional force is found to be maximum at 6 kW and ~~be~~ minimum at 12 kW operating power. At 15 kW of operating power, the frictional force was ~~reported~~ found to be in the range of values ~~whatever lies~~ for the power levels ~~in~~ between 9 to 12 kW. These results are in accordance with the findings ~~as being~~ observed for wear rates.

Wear morphology for selected coating samples ~~were being~~are highlighted in some images captured by FESEM. Figure 10 represents the wear morphological images for red mud with 10% fly ash coating (prepared at 6 kW operating power) allowed for sliding for the time intervals of 3, 6, 12 and 15 minutes. Owing to continuous sliding of counter surfaces, wear debris formed which interlock~~s~~ within the sliding interfaces, caus~~attribut~~ing pitting and eventually crack formation. Wear scars, debris formed and cracked sections are ~~being~~ clearly visible in Figure 10 (b) and ~~Fig 10~~ (d), ~~assigning to~~indicating a fatigue failure ~~in the real sense~~ on the worn surface. Figure 11 shows the worn surfaces for 50 % fly ash based red mud coatings (prepared at 12 kW of operating power level) for the sliding intervals 3, 6, 12, 15, 27 and 30 minutes. The wear morphology changes with increase in the sliding distance, impacting change in surface roughness, leading to the interruption of its contact mechanism. The change in wear characteristics may be attributed ~~due~~ to the variation of hardness of coating inter-layers with respect to the change in sliding distance. At incipient, a slow increase in wear rate is observed and then attains a rapid increment, the ‘break in’ situation, after traversing of certain sliding distance. The further increase in sliding distance cannot change the contact area; causing a relatively steady wear rate. Hence, it can be concluded that the wear takes place by the phenomenon of adhesion and abrasive mechanism due to development of shear stresses ~~in~~ between the hard asperities of the two surfaces in contact. After the “break in” phase, the trend of wear rate remains almost constant for coatings deposited at all power levels. The duration of this stage extends till the end of the test.

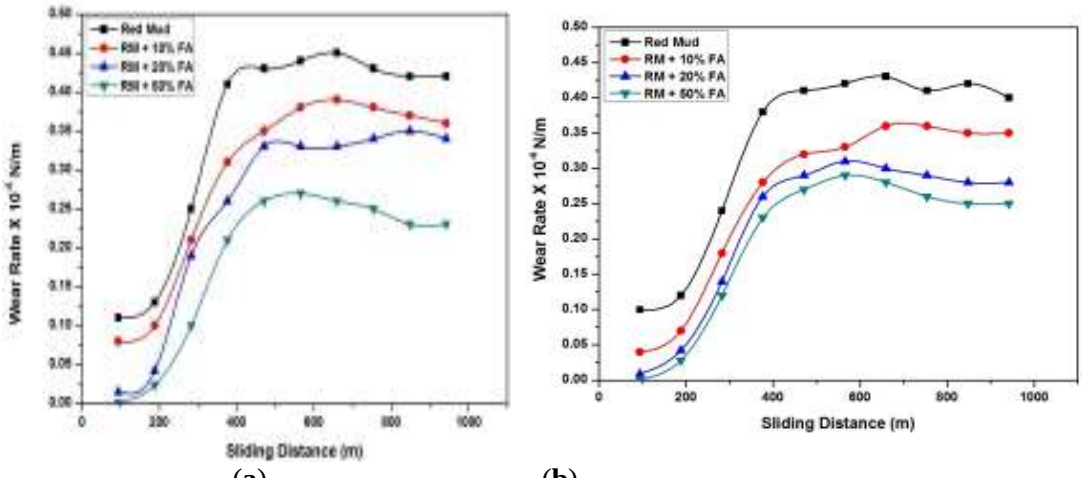

(**a**) (**b**)

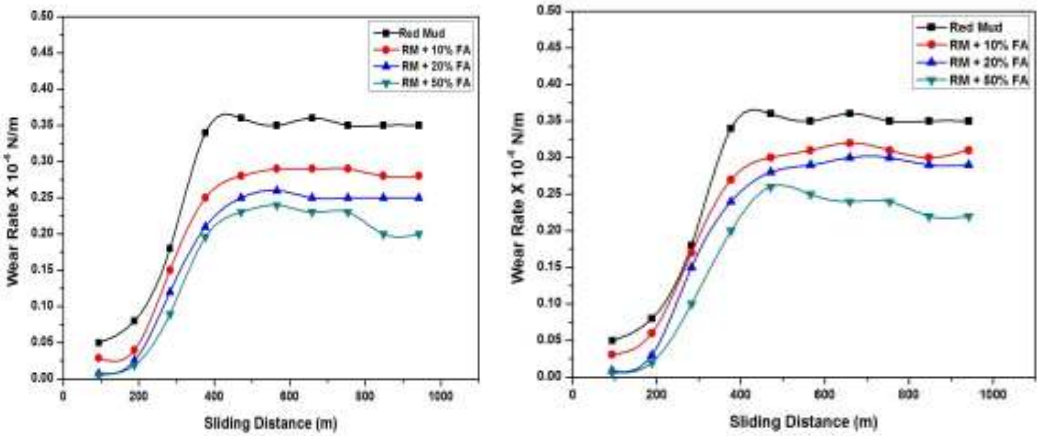

(c) **(d)**

Figure 5. Wear rates obtained for different coating type with sliding distance. (a) 6 kW, (b) 9 kW, (c) 12 kW, (d) 15 kW.

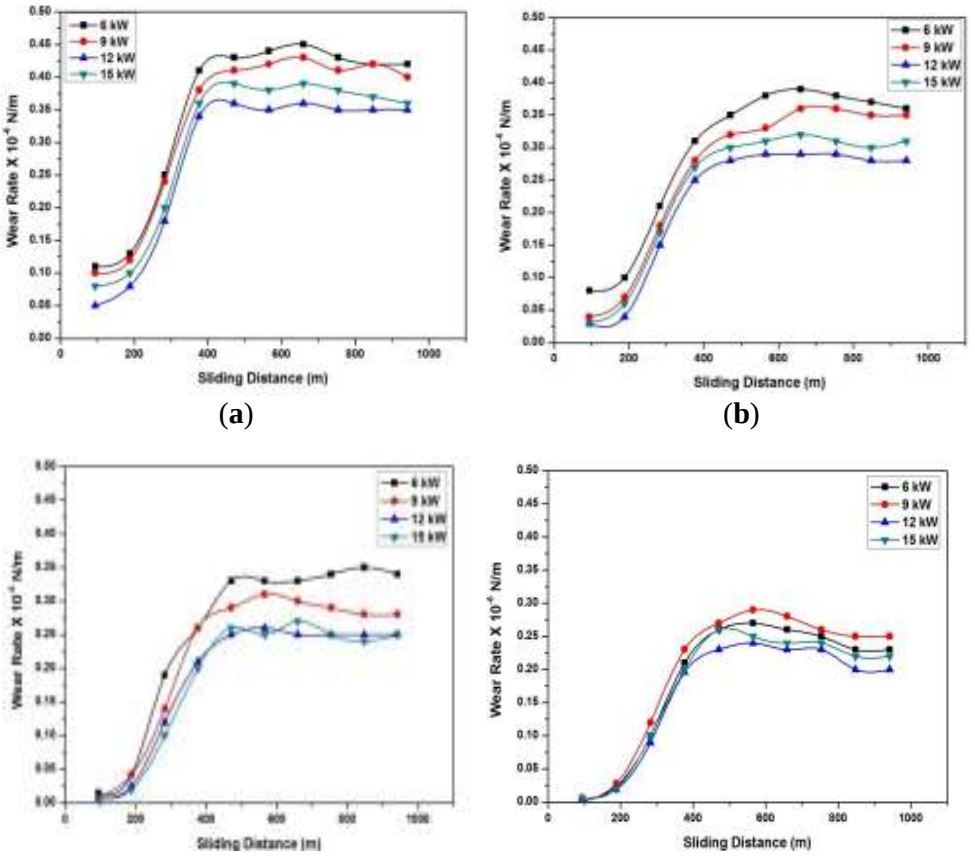

Figure 6. Wear rate comparison for different operating power level. (a) ~~Red Mud~~red mud, (b) ~~Red Mud~~red mud +10 % ~~Fly Ash~~fly ash, (c) ~~Red Mud~~red mud+20% ~~Fly Ash~~fly ash, (d) ~~Red Mud~~red mud+50% ~~Fly Ash~~fly ash.

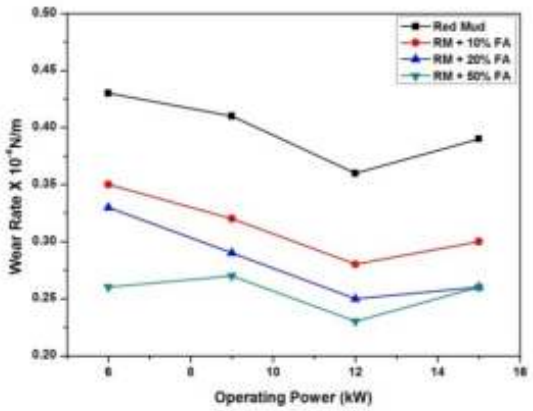

Figure 7. Variation of wear rate with operating power level at sliding time of 15 minutes.

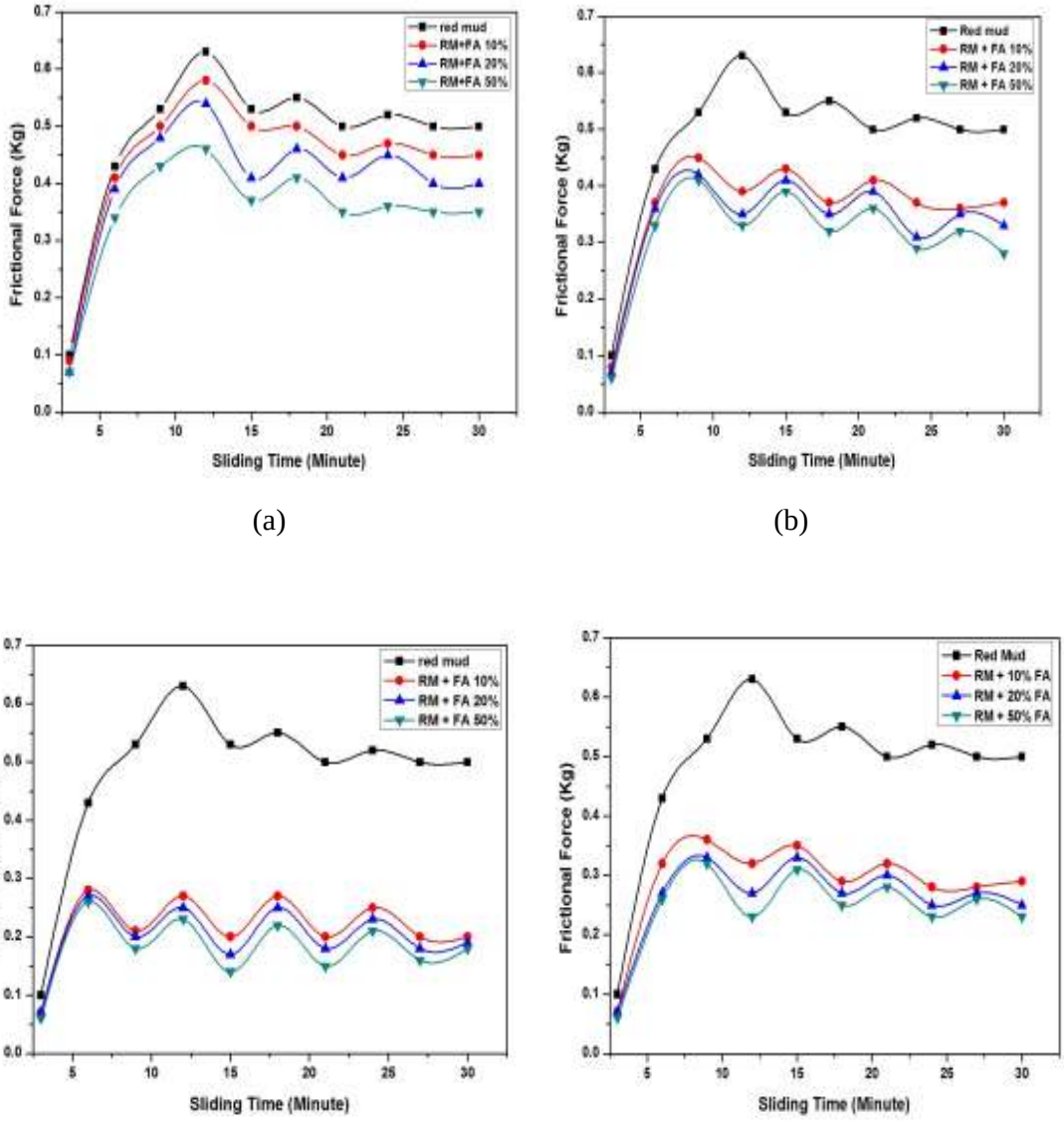

Figure 8. Frictional forces against sliding time for all coating type. (a) 6 kW, (b) 9 kW, (c) 12 kW, (d) 15 kW.

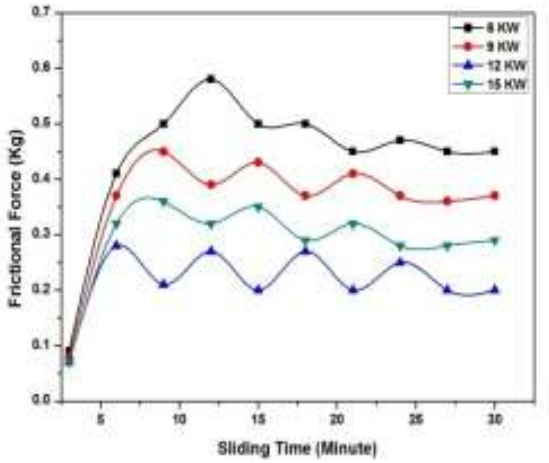

Figure ~~.~~ 9. Comparison of frictional force values for 10 % fly ash coating.

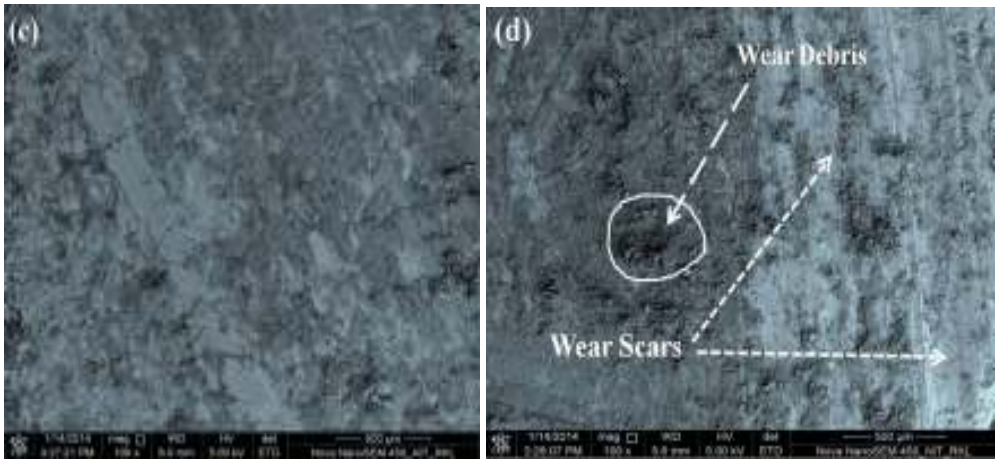

Figure ~~.~~10. Worn s~~S~~urfaces for ~~Red Mud~~red mud + 10 % f~~F~~ly ash coatings for 6 kW o~~O~~perating p~~P~~ower l~~L~~evel~~.~~; (a) 3, (b) 6, (c) 12 and (d) 15 minutes time interval.

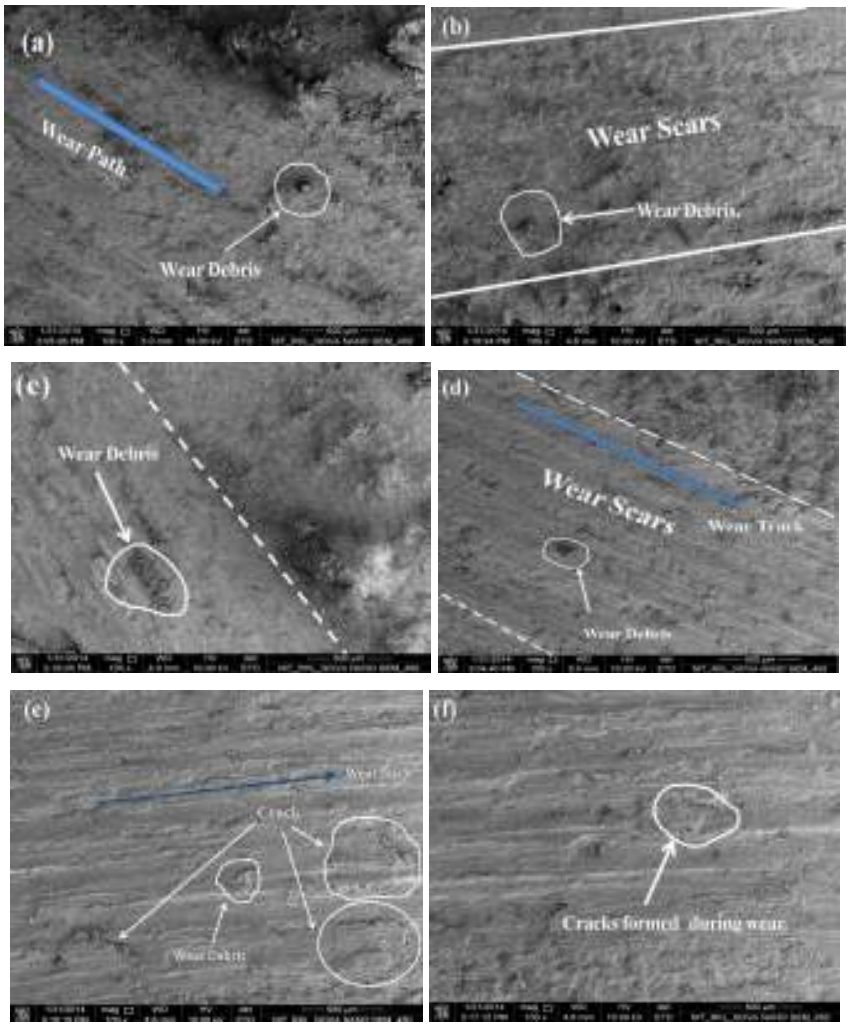

Figure.11. Worn sSurfaces for ~~Red Mud~~red mud + 50 % fF~~~~ly ash coatings for 12 kW oO~~~~perating pP~~~~ower lL~~~~evel~~.~~; (a) 3, (b) 6, (c) 12 ,(d)15, (e) 27 and (f) 30 minutes time intervals.

4. CONCLUSION

The present experimental investigations ~~are being winded up with~~allow for some salient concluding remarks. Red mud, the waste generated from alumina plants is ~~eminently~~ coat~~-~~able on metal substrates by employing thermal plasma spraying technique with excellent wear resistance. The addition of fly ash with red mud reduces the wear rate by enhancing the coating property. But the optimum percentages of fly ash required for better coating material still impact a question mark for the researchers. It is observed that for the early stage, the wear rate increases slowly and then rises drastically ~~improved~~ with sliding distance for all coating types and finally becomes stagnant. Operating power level proved to be the remarkable variable for coating property.~~; which enhances~~ The~~t~~he coating wear resistance~~, but afterwards with reaching~~ increases until ~~-~~an optimum value at 12 kW, indicating some other dominating

parameters. The present work leaves ~~with some~~a wide spectrum of scopes for future investigators to explore many other aspects of red mud coatings. Thermal stability of these coatings may be evaluated for better claiming in high temperature applications. Corrosive wear behavior under different operating conditions may be investigated to identify suitable application areas. Post heat treatment of these coatings may also be implemented ~~further~~ for furthering the study regarding the improvement in coating quality and properties.

CONFLICT OF INTEREST

The authors declare no conflict of interest exist for publishing this paper.

References

1. Kushner, B.A., and Novinski, E.R. "Thermal spray coating," *ASM Hand–book*, **18** (829-833).1992.
2. Crook, P.; "Friction and wear of Hard facing Alloy," *ASM Hand-book*, **18** (758-765), 1992.
3. Mishra, S.C., Das, S., Satapathy, A.~~lok.~~, Ananthapadmanabhan, P.V., and Sreekumar, K.P., "Erosion Wear Analysis of Plasma Sprayed Ceramic Coating Using the Taguchi Technique," *Tribology Transactions*, 2009, vol.52, no.3, pp. 401-404.
4. Ay, N., Nuri Çelik, O., and Göncü, Y., "Wear Characteristics of Traditional Manganese Phosphate and Composite hBN Coatings," *Tribology Transactions*, 2013, vol.56, no.6, pp 1109-1118.
5. Afzal, M., Ajmal, M., and Khan, A. N., "Wear Behavior of WC-12% Co Coatings Produced by Air Plasma Spraying at Different Standoff Distances," *Tribology Transactions*, 2014, vol.57, no.1, pp 94-103.
6. Wayne~~a~~, S.F., Sampath., S. and Anand, V., "Wear Mechanisms in Thermally Sprayed Mo-Based Coatings", *Tribology Transactions*, 1994, vol.**37**, no.3, pp :636-640.
7. Wang, Y., Jin, Y. and Wen, S., "The analysis of the friction and wear mechanisms of plasma-sprayed coatings at 450°C," *Wear*, 1998, vol.**128** , pp. 265–276.
8. Wang, Y., Jin, Y. and Wen, S., "The analysis of the chemical structure and properties of ceramic surface films in friction using SEM, AES and Micro-region X-ray diffraction," *Wear*, 1998, vol.**128**, pp. 277–290.
9. Wang, Y., Jin, Y. and Wen, S., "The inspection of sliding surface and subsurface of plasma-sprayed using scanning acoustic microscopy," *Wear*, 1998, vol.**134**, pp. 399–411.
10. Vijande-Diaz, R., Belzunce, J., Fernandez, E., Rincon, A. and Pérez, M.C.,Wear and microstructure in fine ceramic coatings, *Wear*, 1991,vol.**148**, pp. 233–331.
11. Wei, J. and Xue, Q., "Effects of additives on friction and wear behaviour of Cr_2O_3 coatings," *Wear*, 1993, vol.**160**, pp. 61–65.
12. Homberg, K., Mathews, A. and Ronkainen, H., "Coatings Tribology-Contact mechanisms and surface design," *Tribology International*,1998, **31**(1-3), pp 107-120.

13. Sutar, H., Mishra, S.C., Sahoo, S.K., Chakraverty, A.P. and Maharana, H.S., "Progress of Red Mud Utilization: An Overview," *American Chemical Science Journal*, 2014 , vol.4,no.3, pp 255-279.
14. Sutar, H., Mishra, S.C., Sahoo, S.K., Satapathy, A. and Kumar, V., "Morphology and solid particle erosion wear behaviour of red mud composite coatings." *Natural Science*, 2012,vol.4, no.11, 832-838.
15. Satapathy, A., Sutar, H., Mishra, S.C and Sahoo, S.K, "Characterization of Plasma Sprayed Pure Red Mud Coatings: An Analysis," *American Chemical Science Journal*, 2013, vol.3 no.2, pp 151-163.
16. Prasad, N., Sutar, H., Mishra, S.C., Sahoo, S.K and Acharya, S.K, "Dry sliding wear behavior of aluminium matrix composite using red mud an industrial waste," *International Research Journal of Pure and Applied Chemistry*,2013, vol.3,no.1, pp 59-74.
17. Sutar, H., Mishra, S.C., Sahoo, S.K., Maharana, H.S. and Chakraverty, A.P., "–Tribological Aspects of Thermally Sprayed Red Mud-Fly Ash and Red Mud-Al Coatings on Mild Steel" *American Chemical Science Journal,* 2014 , vol.4, no.6, pp 1014-1031..
18. Pawlowski, L, "The Science and Engineering of Thermal Spray Coatings," John Wiley and Sons, New York , pp. 218, 1995.
19. Satapathy, A., "Thermal Spray Coating of Red mud on Metals" *PhD Thesis*, National Institute of Technology, Rourkela, Odisha, India, 2005.